Chiral condensate from renormalization group optimized perturbation

Jean-Loïc Kneur and André Neveu

Laboratoire Charles Coulomb (L2C), UMR 5221 CNRS-Université de Montpellier, 34095 Montpellier, France

(Received 1 July 2015; published 21 October 2015)

Our recently developed variant of variationally optimized perturbation, in particular consistently incorporating renormalization group properties, is adapted to the calculation of the QCD spectral density of the Dirac operator and the related chiral quark condensate $\langle\bar{q}q\rangle$ in the chiral limit, for $n_f = 2$ and $n_f = 3$ massless quarks. The results of successive sequences of approximations at two-, three-, and four-loop orders of this modified perturbation exhibit a remarkable stability. We obtain $\langle\bar{q}q\rangle^{1/3}_{n_f=2}(2\ \mathrm{GeV}) = -(0.833\text{–}0.845)\bar{\Lambda}_2$, and $\langle\bar{q}q\rangle^{1/3}_{n_f=3}(2\ \mathrm{GeV}) = -(0.814\text{–}0.838)\bar{\Lambda}_3$ where the range spanned by the first and second numbers (respectively, four- and three-loop order results) defines our theoretical error, and $\bar{\Lambda}_{n_f}$ is the basic QCD scale in the $\overline{\mathrm{MS}}$ scheme. We obtain a moderate suppression of the chiral condensate when going from $n_f = 2$ to $n_f = 3$. We compare these results with some other recent determinations from other nonperturbative methods (mainly lattice and spectral sum rules).

DOI: 10.1103/PhysRevD.92.074027 PACS numbers: 12.38.Aw, 12.38.Cy, 12.38.Lg

I. INTRODUCTION

The chiral quark condensate $\langle\bar{q}q\rangle$ plays a central role in QCD nonperturbative dynamics, and it is one of the principal (lowest-dimensional) order parameters of spontaneous chiral symmetry breaking, $\mathrm{SU}(n_f)_L \times \mathrm{SU}(n_f)_R \to \mathrm{SU}(n_f)_V$ for n_f massless quarks (the other being the pion decay constant), where the physically relevant cases are $n_f = 2$ or 3. It is considered a nonperturbative quantity by excellence, in the sense that it is trivially vanishing at any finite order of (ordinary) perturbative QCD in the chiral (massless quark) limit, as we recall in more detail below.

There is a long history of its determination from various models and analytic methods, the best known being the Gell-Mann–Oakes–Renner (GMOR) relation [1] relating the quark condensate to the pion mass, the decay constant F_π, and the light current quark masses $m_{u,d}$, typically for the degenerate two-flavor case:

$$F_\pi^2 m_\pi^2 = -(m_u + m_d)\langle\bar{u}u\rangle + \mathcal{O}(m_q^2). \tag{1.1}$$

Nowadays the light current quark masses can be precisely extracted from lattice simulations [2] or spectral sum rules (see, e.g., Ref. [3]), with the GMOR relation above giving an indirect precise determination of the condensate. However, as indicated Eq. (1.1) is valid upon neglecting possible higher-order terms $\mathcal{O}(m_q^2)$. Indeed, the GMOR relation entails explicit chiral symmetry breaking from current quark masses. Since the condensate is more a property of the QCD vacuum in the strict chiral limit, it is highly desirable to obtain a possible "first-principle" determination of this dynamical quantity in the strict chiral limit, to disentangle it from quark current mass effects. An early analytic determination was in the framework of the Nambu–Jona-Lasinio (NJL) model [4] and its various extensions as a low-energy effective model of QCD, valid at least for the gross features of chiral-symmetry-breaking properties. In the NJL model, the condensate is evaluated in the strict chiral limit, or by taking into account explicit breaking from small current quark masses, in the leading (large-N) approximation [5] as a function of the physical cutoff and other parameters of the model to be fitted from data. There have are also been other related attempts based on analytic methods like the Schwinger-Dyson equations [6,7]. Phenomenological values of the condensate can also be extracted [3,8] indirectly from data using spectral QCD sum rule methods [9], where the quark condensate and other higher-dimensional condensates enter as nonperturbative parameters of the operator product expansion in inverse powers of momenta.

More recently, *ab initio* lattice calculations have determined the quark condensate using several independent approaches; some are actually related to the GMOR relation, while others are more direct determinations that use different methods [10] (see Ref. [2] for a review of various recent lattice determinations). In particular, after early pioneering work [11], there has been more recently a renewed intense interest in computing the spectral density of the Dirac operator on the lattice [12,13], which is directly related to the quark condensate through the Banks-Casher relation [14]. However, while many recent lattice results are statistically very precise, lattice determinations rely in the end on extrapolations to the chiral limit, often using chiral perturbation theory [15] input for that purpose. Earlier general results on the spectral density in the nonperturbative low-eigenvalue range were obtained in Ref. [16], and

attempts to use chiral perturbation theory information was elaborated, e.g., in Ref. [17]. The link between different definitions of the quark condensate—in particular, between the spectral density and the condensate appearing in the operator product expansion—was carefully discussed in Ref. [7].

On more phenomenological grounds, there are also long-standing questions on the dependence of the quark condensate on the number of flavors ($n_f = 2$ or $n_f = 3$ for the physically relevant cases). In particular, it has been advocated that the GMOR relation may receive substantial corrections, and some authors indeed found significant suppression of the three-flavor case with respect to the two-flavor case [18], which may be attributed to the relatively large explicit chiral breaking from the not-so-small mass of the strange quark, roughly of order $m_s\bar{\Lambda}_{\rm QCD}/3$. There are also some hints that chiral perturbation theory might not converge very well for $n_f = 3$ [18,19], for which value lattice simulations also show large discrepancies between different collaborations and methods (with some results with, and some other results without relative suppression of the $n_f = 3$ condensate [2]).

Our recently developed renormalization group optimized perturbation (RGOPT) method [20–22] appears particularly adapted to estimate this quantity, since it gives a nonperturbative sequence of approximations starting from a purely perturbative expression. This allows by construction an analytic "first-principle" calculation of this quantity and gives a nontrivial result by construction in the chiral limit, in contrast with the standard perturbative one (see also Refs. [23,24] for earlier attempts in that direction). Moreover, this also gives us a very simple analytic handle on the exploration of the chiral limit for an arbitrary number of flavors (two or three in practice), which in our framework is simply contained in the known flavor dependence of the first few perturbative coefficients, while this appears more difficult at present both for chiral perturbation theory and lattice simulations.

The paper is organized as follows. In Sec. II we shortly recall the basics of the spectral density and its Banks-Casher connection with the condensate. In Sec. III we recall the main OPT method and our RGOPT version incorporating consistent RG properties. We adapt the RGOPT to the spectral density case in Sec. III. C. Section IV is a digression where we first consider the spectral density RGOPT calculation in the Gross-Neveu model, where it can be compared with the exact result for the fermion condensate in the large-N limit, known from standard methods. Section V deals with the actual computation of the optimized spectral density in QCD at the three presently available orders (two, three, and four loops) of the variationally modified perturbation. Detailed numerical results are presented as well as some comparison with other recent determinations of the quark condensate. Finally, Sec. VI is a conclusion.

II. SPECTRAL DENSITY AND THE QUARK CONDENSATE

We shall just recall in this section some rather well-known features of the spectral density and its connection with the chiral condensate, known as the Banks-Casher relation [14] (see also, e.g., Ref. [16] for more details), to be exploited below. We thus start from the (Euclidean) Dirac operator which formally has eigenvalues λ_n and eigenvectors u_n,

$$\mathrm{i}\not{D}u_n(x) = \lambda_n u_n(x); \qquad \not{D} \equiv \not{\partial} + g\not{A}, \tag{2.1}$$

where $\not{D}$ is the covariant derivative operator and A the gluon field. Except for zero modes, the eigenvectors come in pairs $\{u_n(x); \gamma_5 u_n(x)\}$, with respective eigenvalues $\{\lambda_n; -\lambda_n\}$ that depend on A. In the discrete case (i.e., on a lattice with finite volume V), by definition the spectral density is given by

$$\rho(\lambda) \equiv \frac{1}{V}\left\langle \sum_n \delta(\lambda - \lambda_n^{[A]}) \right\rangle, \tag{2.2}$$

where $\delta(x)$ here is the Dirac distribution and $\langle\cdots\rangle$ designates averaging over the gauge field configurations,

$$\langle\rangle = \int [\mathrm{d}A] \prod_{i=1}^{N} \det(\mathrm{i}\not{D} + m). \tag{2.3}$$

The quark condensate is given by

$$\frac{1}{V}\int_V \mathrm{d}^4x \langle\bar{q}(x)q(x)\rangle = -2\frac{m}{V}\sum_{\lambda_n>0}\frac{1}{\lambda_n^2 + m^2}. \tag{2.4}$$

Now when V goes to infinity the operator spectrum becomes dense, so that

$$\langle\bar{q}q\rangle = -2m\int_0^\infty \mathrm{d}\lambda \frac{\rho(\lambda)}{\lambda^2 + m^2}, \tag{2.5}$$

where $\rho(\lambda)$ is the spectral density.

The Banks-Casher relation is the $m \to 0$ limit of this, giving the condensate in the relevant chiral-symmetric limit as

$$\lim_{m\to 0}\langle\bar{q}q\rangle = -\pi\rho(0) \tag{2.6}$$

if the spectral density at the origin can be known. This is an intrinsically nonperturbative quantity, vanishing to all orders of ordinary perturbation, just as the left-hand side of this last equation. Now taking into account that for nonzero fermion masses m, $\langle\bar{q}q\rangle = \langle\bar{q}q\rangle(m) \equiv -\Sigma(m)$, we have from the defining relations (2.2) and (2.5) the following interesting tautology:

$$\rho(\lambda) = \frac{1}{2\pi}[\Sigma(\mathrm{i}\lambda+\epsilon) - \Sigma(\mathrm{i}\lambda-\epsilon)]|_{\epsilon\to 0}, \qquad (2.7)$$

i.e., $\rho(\lambda)$ is determined by the discontinuities of $\Sigma(m)$ across the imaginary axis. This relation is interesting because, when the quark mass is nonzero, $\langle\bar{q}q\rangle$ has a purely perturbative series expansion, known to three-loop order at present, and its discontinuities are simply given by those coming from the perturbative, purely logarithmic mass dependence. Therefore it makes sense to calculate a perturbative spectral density using the above relation. Usually it will be of little use, since taking its $\lambda \to 0$ limit (which is relevant for the true chiral condensate) will only lead to a trivially vanishing result [7]. But the OPT (and in particular our RGOPT version) series modification after performing the variational δ expansion (see below) is precisely the analytic handle giving a nontrivial result for $\lambda \to 0$, just as it gives a nontrivial result for $m \to 0$ for modified perturbative series with mass dependence.

Thus the recipe we shall apply is clear. In a first stage we calculate the purely perturbative expression of $\rho(\lambda)$ up to four loops, using the logarithmic discontinuities involved in Eq. (2.7). Then, we perform a variational transformation (the so-called δ expansion, defined in the next section) on the perturbative series, and solve appropriate OPT and RG equations (to be precisely defined in the next section) to derive a nontrivial, optimized value of Eq. (2.6).

III. OPTIMIZED AND RG-OPTIMIZED PERTURBATION

A. Standard OPT

The key feature of the OPT method (appearing in the literature under many names and variations [25]) is to introduce an extra parameter $0 < \delta < 1$, interpolating between $\mathcal{L}_{\text{free}}$ and $\mathcal{L}_{\text{int}}$ for any Lagrangian, in such a way that the mass parameter m is traded for an arbitrary trial parameter. This is perturbatively equivalent to taking any standard perturbative expansions in the coupling $g(\mu)$, after renormalization in some given scheme (e.g., the modified minimal subtraction ($\overline{\text{MS}}$) scheme with arbitrary scale μ), reexpanded in powers of δ after substituting

$$m \to m(1-\delta)^a, \qquad g \to \delta g. \qquad (3.1)$$

Such a procedure is consistent with renormalizability [23,24,26] and gauge invariance [24], whenever the latter is relevant, provided of course that the above redefinition of the coupling is performed consistently for all interaction terms and counterterms appropriate for renormalizability and gauge invariance, as is the case for QCD. In Eq. (3.1) we introduced an extra parameter a to reflect a certain freedom in the interpolation form, which will be crucial to impose compelling RG constraints, as discussed below and in our previous work [21,22]. Applying Eq. (3.1) to a given perturbative expansion for a physical quantity $P(m,\lambda)$, reexpanded in δ at order k, and taking *afterwards* the $\delta \to 1$ limit to recover the original *massless* theory, leaves a remnant m dependence at any finite δ^k order. The arbitrary mass parameter m is then most conveniently fixed by an optimization prescription,

$$\frac{\partial}{\partial m} P^{(k)}(m,g,\delta=1)|_{m\equiv\tilde{m}} = 0, \qquad (3.2)$$

which generally determines a nontrivial optimized mass $\tilde{m}(g)$, having a nonperturbative g dependence, realizing dimensional transmutation. (More precisely, for asymptotically free theories, the optimized mass is automatically of the order of the basic scale $\Lambda \sim \mu e^{-1/(b_0 g)}$, in contrast with the original vanishing mass.) In simpler ($D = 1$) models the procedure may be seen as a particular case of "order-dependent mapping" [27], which has been proven [28] to converge exponentially fast for the $D = 1$ Φ^4 oscillator energy levels. For higher-dimensional $D > 1$ renormalizable models, the behavior at large orders in δ is more involved, and no rigorous convergence proof exists, although OPT was shown to partially damp the factorially divergent (infrared renormalons) perturbative behavior at large orders [29]. Nevertheless, the OPT can give rather successful approximations for nonperturbative quantities beyond mean-field approximations in a large variety of models [25,30,31], including studies of phase transitions at finite temperatures and densities [32,33].

B. Renormalization-group-optimized perturbation

In most previous OPT applications [25], the linear δ expansion was used, namely assuming $a = 1$ in Eq. (3.1) mainly for simplicity and economy of parameters. However, a well-known drawback of this conventional OPT approach is that, beyond lowest order, Eq. (3.2) generally gives more and more solutions at increasing orders, many being complex valued, as a result of exactly solving algebraic equations in g and/or m. This problem is typically encountered first at two-loop order. In general, without some insight on the nonperturbative behavior of the solutions, it can be difficult to select the right one, and unphysical nonreal solutions at higher orders are embarrassing. As it turns out, RG consistency considerations provide a compelling way out, as developed in our more recent approach [20–22], which differs crucially from the more conventional OPT based on the linear δ expansion in two main respects. First, it introduces a straightforward combination of OPT and RG properties, by requiring the (δ-modified) expansion to satisfy, in addition to the OPT (3.2), a standard RG equation,

$$\mu\frac{\mathrm{d}}{\mathrm{d}\mu}(P^{(k)}(m,g,\delta=1)) = 0, \qquad (3.3)$$

where the RG operator is defined as usual,[1]

$$\mu\frac{\mathrm{d}}{\mathrm{d}\mu}=\mu\frac{\partial}{\partial\mu}+\beta(g)\frac{\partial}{\partial g}-\gamma_m(g)m\frac{\partial}{\partial m}. \tag{3.4}$$

Note, once combined with Eq. (3.2), the RG equation takes a reduced simple form, corresponding to a massless theory,

$$\left[\mu\frac{\partial}{\partial\mu}+\beta(g)\frac{\partial}{\partial g}\right]P^{(k)}(m,g,\delta=1)=0. \tag{3.5}$$

Thus Eqs. (3.5) and (3.2) together completely fix *optimized* $m\equiv\tilde{m}$ and $g\equiv\tilde{g}$ values.

Indeed, we remark that RG invariance is in general spoiled after the rather drastic modification from Eq. (3.1), reshuffling interaction and free terms from the original perturbative expansion. This feature has seldom been considered and appreciated in previous applications of the OPT based on the linear δ-expansion method to renormalizable theories. Thus RG invariance has to be restored in some manner; accordingly, Eq. (3.5) gives an additional nontrivial constraint. Intuitively, just as the stationary point OPT solutions from Eq. (3.2) are expected to give sensible approximations (at successive orders) to the actually massless theory, one similarly expects that combining the OPT with the RG solutions of Eq. (3.5) should further give a sensible sequence of best approximations to the exactly scale-invariant all-order result. [N. B.: An earlier way of reconciling the δ expansion with RG properties was used in Refs. [23,24,26]. Schematically it amounted to resumming the δ expansion to all orders, which can be done in practice only for the pure RG dependence up to two-loop order. These resummations came as rather complicated integral representations, rendering difficult generalizations to higher orders, other physical quantities, or other models of interest. In contrast, the purely perturbative procedure of imposing Eqs. (3.2) and (3.5) is a considerable shortcut, and it is straightforward to apply to any model as it is based solely on purely perturbative expansions.]

Yet applying Eqs. (3.2) and (3.5) without further insight still gives multiple solutions at increasing orders. So we proposed [21,22] a compelling selection criterion by retaining only the branch solution(s) $g(m)$ [or equivalently $m(g)$] *continuously matching* the standard perturbative approach [asymptotically free (AF) RG behavior in the QCD case] for vanishing coupling, namely,

$$\tilde{g}(\mu\gg\tilde{m})\sim\left(2b_0\ln\frac{\mu}{\tilde{m}}\right)^{-1}+\mathcal{O}\left(\left(\ln\frac{\mu}{\tilde{m}}\right)^{-2}\right). \tag{3.6}$$

Now the crucial observation is that requiring at least one of the solutions of Eq. (3.5) to satisfy Eq. (3.6) implies a strong necessary condition on the basic interpolation (3.1), fixing the exponent a uniquely in terms of the universal (scheme-independent) first-order RG coefficients [21,22],

$$a\equiv\frac{\gamma_0}{2b_0}, \tag{3.7}$$

which is the second important difference of the present RGOPT with respect to the standard OPT.[2] For the critical value (3.7), Eq. (3.5) is in fact exactly satisfied at the lowest δ^0 order, therefore giving no further constraint. At higher δ orders, Eq. (3.7) implies that at least one of the RG and OPT solutions fulfills Eq. (3.6), and solutions with this behavior are essentially unique (although not necessarily) at a given perturbative order. Moreover, taking Eq. (3.7) drastically improves the convergence of the method; more precisely, the known nonperturbative result of generic pure RG-resummed expressions are obtained exactly from RGOPT at the very first δ order, while the convergence of the conventional OPT with $a=1$ is not clear or very slow, if it occurs at all (see Sec. III. C of Ref. [22] for details).

The criterion (3.6) can easily be generalized to any model, even nonasymptotically free ones, by similarly selecting those optimized solutions that simply match the standard perturbative behavior for small coupling values. Thus, clearly the resulting unique critical value like in Eq. (3.7) is valid for any model with its appropriate RG coefficients. For the QCD spectral density (as we will see below) the equivalent of the criteria (3.6) indeed selects a unique solution at a given order for both the RG and OPT equations, at least up to the four-loop order (as was also the case for the pion decay constant [22]).

Incidentally, a connection of the exponent a with RG anomalous dimensions/critical exponents had also been established previously in a different context, in the $D=3$ Φ^4 model for the Bose-Einstein condensate critical temperature shift, by two independent approaches [30,31], where for this model it also leads to real OPT solutions [31]. Indeed, in Refs. [30,35] it was convincingly argued, based on critical behavior considerations, that the OPT can only converge if an appropriate Wegner critical exponent is used in the interpolation (3.1), which appears quite similar to our criterion (3.7). Note however that Eq. (3.7) is identified exactly from the known first-order RG coefficients, and thus it is valid for any model, while in Ref. [35] the analogous exponent was determined more approximately by looking for a plateau in the variational parameter

[1]For QCD our normalization is $\beta(g)\equiv dg/d\ln\mu=-2b_0g^2-2b_1g^3+\cdots$, $\gamma_m(g)=\gamma_0g+\gamma_1g^2+\cdots$, where $g\equiv4\pi\alpha_S$. The b_i, γ_i coefficients up to four loops are given in Ref. [34].

[2]The important role of the anomalous dimension $\gamma_0/(2b_0)$ appeared also in our earlier constructions that resummed the RG dependence of the δ expansion [23,24,26,29], although it had not been recognized at that time as a crucial RG consistency property of lowest δ orders.

dependence. In any case, from these examples it is established that it is necessary for the OPT method to give useful results to have in general an exponent a in Eq. (3.1) differing from 1 in a well-defined way.

Coming back to the present OPT and RG equations (3.2) and (3.5), beyond lowest orders AF-compatible solutions with behavior like Eq. (3.6) are however not necessarily real in general. A rather simple way out is to further exploit the RG freedom, considering a perturbative renormalization scheme change to attempt to recover RGOPT solutions that are both AF compatible and real [22]. In the present case of the spectral density, this extra complication is not even necessary, at least up to the highest order studied here (four loops): we shall also find that the unique AF-compatible RG and OPT solution remains real.

C. RGOPT for the spectral density

Formally, a generic perturbative expansion for the condensate typically reads

$$\langle\bar{q}q\rangle_{\rm pert} = m^3\sum_p g^p \sum_{k=0}^{p} f_{pk}\ln^{p-k}\left(\frac{m}{\mu}\right), \tag{3.8}$$

where the f_{pk} coefficients are determined by RG properties from the lowest orders for $k < p$. According to Eq. (2.7), calculating the (perturbative) spectral density formally involves calculating all logarithmic discontinuities. This is conveniently given [in any typical perturbative expansion like Eq. (3.8)] by taking all nonlogarithmic terms to zero—those trivially having no discontinuities—while replacing all powers of logarithms, using $m \to {\rm i}|\lambda|$, etc., as

$$\begin{aligned}\ln^n\left(\frac{m}{\mu}\right) &= \frac{1}{2^n}\ln^n\left(\frac{m^2}{\mu^2}\right)\\ &\to \frac{1}{2^n}\frac{1}{2{\rm i}\pi}\left[\left(2\ln\frac{|\lambda|}{\mu}+{\rm i}\pi\right)^n-\left(2\ln\frac{|\lambda|}{\mu}-{\rm i}\pi\right)^n\right],\end{aligned} \tag{3.9}$$

leading to the following simple substitution rules for the first few terms:

$$\begin{aligned}&\ln\left(\frac{m}{\mu}\right)\to 1/2; \qquad \ln^2\left(\frac{m}{\mu}\right)\to \ln\frac{|\lambda|}{\mu};\\ &\ln^3\left(\frac{m}{\mu}\right)\to\frac{3}{2}\ln^2\frac{|\lambda|}{\mu}-\frac{\pi^2}{8},\end{aligned} \tag{3.10}$$

and so on (note the appearance of nonlogarithmic $\sim\pi^2$ terms starting at order $\ln^3 m$). This gives a perturbative expression of the spectral density of the generic form

$$\rho_{\rm pert}(|\lambda|,g) = |\lambda|^3\sum_{p\geq 1} g^p\sum_{k=0}^{p} f^{\rm SD}_{pk}\ln^{p-k}\left(\frac{|\lambda|}{\mu}\right), \tag{3.11}$$

where the determination of the coefficients $f^{\rm SD}_{pk}$ follows from the above relations (3.9). To obtain the RG equation for $\rho(g,\lambda)$, we use the defining integral representation of the spectral density in Eq. (2.5) and the basic algebraic identity

$$\frac{\partial}{\partial m}\frac{m}{\lambda^2+m^2} = -\frac{\partial}{\partial\lambda}\frac{\lambda}{\lambda^2+m^2}. \tag{3.12}$$

Throwing away surface terms in partial integrations (as is usually done in the spirit of dimensional regularization), one thus finds that $\rho(\lambda)$ actually obeys the same RG equation as $\langle\bar{q}q\rangle$, with ∂m replaced by $\partial\lambda$,

$$\left[\mu\frac{\partial}{\partial\mu}+\beta(g)\frac{\partial}{\partial g}-\gamma_m(g)\lambda\frac{\partial}{\partial\lambda}-\gamma_m(g)\right]\rho(\lambda,g)=0. \tag{3.13}$$

One can next proceed to the modification of the resulting perturbative series $\rho(\lambda,g)$ as implied by the δ expansion, which [from Eq. (3.12)] is now clearly applied not on the original mass but on the spectral value[3] λ:

$$\lambda\to\lambda(1-\delta)^a \; g\to\delta g. \tag{3.14}$$

Optimizing perturbation theory means that the derivative with respect to m of

$$\sum_{n=0}^{\infty}\frac{(-1)^n}{n!}m^n\left(\frac{\partial}{\partial m}\right)^n\langle\bar{q}q\rangle \tag{3.15}$$

is formally zero,[4] and thus one should obtain a good approximation for the value at $m=0$ of $\langle\bar{q}q\rangle$ at finite order by setting to zero the derivative of a finite number of terms of this series; see Eq. (3.2). Using Eq. (3.12), this mass optimization on $\langle\bar{q}q\rangle$ thus translates into an optimization of the spectral density with respect to λ,

$$\frac{\partial\rho^{(k)}(\lambda,g)}{\partial\lambda}=0, \tag{3.16}$$

at successive δ^k order.

IV. LESSONS FROM THE GROSS-NEVEU MODEL

The fermion condensate can also be defined from the spectral density for the $D=1+1$ $O(N)$ Gross-Neveu (GN) model [36]. This will give us a very useful guidance for the more elaborate QCD case below, and we also set up some formulas that are actually generically valid for both the GN model and QCD.

[3]We adopt in the following the notation $\lambda\equiv|\lambda|$ since it is necessarily positive.

[4]For simplicity, we have set a to one in this equation.

We start from the known expression of the vacuum energy evaluated in the large-N limit [26] after all necessary mass, coupling, and vacuum energy (additive) renormalizations, in terms of the explicit mass m and mass gap $M(m,g)$,

$$E_{\rm GN} = -\left(\frac{N}{4\pi}\right)\left(M^2(m,g) + 2\frac{m}{g}M(m,g)\right), \qquad (4.1)$$

where the mass gap is defined in compact form as

$$M(m,g) = m\left(1 + g\ln\frac{M}{\mu}\right)^{-1}, \qquad (4.2)$$

where $m \equiv m(\mu)$ and $g \equiv g(\mu)$ are the renormalized mass and coupling in the $\overline{\rm MS}$ scheme [after conveniently rescaling the original coupling defined by $(1/2)g_{\rm GN}^2(\bar\Psi\Psi)^2$ as $g_{\rm GN}^2 N/\pi \equiv g$]. The fermion condensate is formally given by the derivative with respect to m of the vacuum energy, giving (after some algebra)

$$\langle\bar\psi\psi\rangle_{\rm GN}(m,g) \equiv -\left(\frac{N}{2\pi}\right)\frac{M(m,g)}{g}. \qquad (4.3)$$

This means that up to a trivial overall factor, the fermion condensate is directly related to the mass gap, as is intuitively expected from mean-field arguments. Equation (4.3) has a well-defined nontrivial perturbative expansion to arbitrary order,

$$\begin{aligned} &-\left(\frac{2\pi}{N}\right)\langle\bar\psi\psi\rangle_{\rm GN}(m,g) \\ &\equiv -\langle\bar\Psi\Psi\rangle_{\rm GN} \\ &\simeq m\left(\frac{1}{g} - L_m + gL_m(L_m+1)\right. \\ &\quad \left. -\frac{1}{2}L_m(L_m+2)(2L_m+1)g^2 + \mathcal{O}(g^3)\right), \end{aligned} \qquad (4.4)$$

where $L_m \equiv \ln m/\mu$ (and for convenience we redefined the condensate by a trivial rescaling). From the properties of the implicit $M(m)$ defined by Eq. (4.2) and its reciprocal function $m(M)$, one can establish [26] that $M(m) \to \Lambda \equiv \mu e^{-1/g}$ for $m \to 0$, which translates here into the simple relation

$$-\langle\bar\Psi\Psi\rangle_{\rm GN}(m \to 0) = \frac{\Lambda}{g}, \qquad (4.5)$$

which provides a consistent bridge between the massive and massless cases. But deriving this requires the knowledge of the all-order expression (4.2), which is only known exactly in the large-N limit.

Now alternatively, performing the substitution[5] (3.1), expanding at order δ^p, setting δ to one, and optimizing the resulting expression with Eqs. (3.2) and (3.5) gives the exact result (4.5) at any order in δ^p, at optimized coupling and mass values,

$$\tilde g = 1; \qquad \tilde L_m = -1, \qquad (4.6)$$

just as in the mass gap case [20]. This is not very surprising, in view of the rather trivial relation (4.5) between the mass gap and the condensate in the large-N limit.

However, here we shall try to obtain this large-N result in an indirect way using the spectral density, with the aim being evidently to test on the exactly known result (4.5) the possibility of calculating a spectral density and of estimating its reliability from the first few perturbative orders, in order to subsequently apply the same procedure in the more challenging QCD case.

Thus from Eq. (4.4) and using $m \to {\rm i}|\lambda|$ and Eq. (3.9), the perturbative expression of the spectral density (for instance, restricted up to four-loop order g^3) is

$$\begin{aligned} \rho_{\rm GN}^{\rm pert}(\lambda,g) \simeq \lambda\left(-\frac{1}{2} + g\left(L_\lambda + \frac{1}{2}\right)\right. \\ -\frac{g^2}{8}(12L_\lambda^2 + 20L_\lambda + 4 - \pi^2) \\ +\frac{g^3}{24}(48L_\lambda^3 + 156L_\lambda^2 + (108 - 12\pi^2)L_\lambda \\ \left. +12 - 13\pi^2) + \mathcal{O}(g^4)\right), \end{aligned} \qquad (4.7)$$

where now $L_\lambda \equiv \ln\lambda/\mu$. We can then proceed by applying Eq. (3.14), expanded to order δ^k, then taking $\delta \to 1$, and finally applying the resulting expression to the OPT (3.16) and RG (3.13) equations. In practice we shall proceed to relatively high perturbative orders, since the exact expression (4.2) may be formally expanded to arbitrary order. Thus with these obvious replacements we can proceed first with the δ expansion (3.14) operating on λ and g, and we take the relevant value of the exponent for the large-N case, $a \equiv \gamma_0/(2b_0) = 1$ in Eq. (3.1). At first nontrivial δ^1 order we simply obtain

$$\rho^{\delta^1}(\delta \to 1;\lambda,g) = \lambda g\left(\frac{1}{2} + L_\lambda\right), \qquad (4.8)$$

from which the OPT (3.16) and RG (3.13) give the unique solution

$$\tilde L_\lambda\left(\equiv \ln\frac{|\lambda|}{\mu}\right) = -\frac{3}{2}; \qquad \tilde g = \frac{1}{2}, \qquad (4.9)$$

[5]Taking $a = 1$ as appropriate for the large-N GN model.

which when plugged back into Eq. (4.8) gives the final result, using also the Banks-Casher relation (2.6),

$$\tilde{g}\langle\bar{\Psi}\Psi\rangle_{\rm GN}(m\to 0)/\Lambda \equiv -\pi\tilde{g}\rho(\tilde{\lambda},\tilde{g})/\Lambda = -\frac{\pi}{4}\sqrt{e}\simeq -1.2949, \qquad (4.10)$$

which is to be compared to the exact result $g\langle\bar{\Psi}\Psi\rangle_{\rm GN}(m\to 0)/\Lambda=-1$ in this normalization. We then proceed to rather high perturbative order, which in practice becomes relatively involved algebraically but can be easily handled with computing software like MATHEMATICA [37]).

The results up to order g^{18} (beyond which numerics become really tedious) are given in Table I (where we give for convenience the scale-invariant condensate $\tilde{g}\langle\bar{\Psi}\Psi\rangle$ values). Actually, starting at order g^3, there is more than one real solution. We show here those solutions which are unambiguously determined to be the closest to the standard AF perturbative behavior, $L_\lambda\simeq -1/g+\mathcal{O}(1)$ for $g\to 0$, by analogy with the exact value $-\tilde{g}\tilde{L}_m\equiv 1$ obtained for the simpler mass gap case. One can see a regular pattern for the values of the optimized coupling for such solutions, with $\tilde{g}\simeq 0.4$, while the optimal spectral parameter $\tilde{L}_\lambda$ is less stable with wider variations at successive orders.

These approximate results at successive orders when optimizing the spectral transform are clearly in contrast with those obtained from directly optimizing the original perturbative expansion, where (as explained above) the AF-compatible solution always gives the exact result for the condensate, with the corresponding optimal coupling and mass values (4.6) obtained already at first and all successive orders. Here we see in Table I that the second order is very close (less than 2%) to the exact result, but at higher orders the solutions exhibit a rather slow empirical convergence, with an oscillating behavior towards the exact large-N limit result.

TABLE I. RGOPT $\frac{-g\langle\bar{\Psi}\Psi\rangle_{\rm GN}}{\Lambda}$, the corresponding optimized coupling $\tilde{g}$, and (the logarithm of) the optimized eigenvalue $\ln\tilde{\lambda}/\mu$ at successive orders in δ.

δ^k order	$\frac{-g\langle\bar{\Psi}\Psi\rangle_{\rm GN}}{\Lambda}$	$\tilde{g}$	$\ln\frac{\tilde{\lambda}}{\mu}$
1	1.295	$\frac{1}{2}$	$-\frac{3}{2}$
2	0.984	0.398	−2.547
3	0.897	0.335	−3.278
4	1.081	0.399	−1.373
5	0.924	0.394	−1.919
6	0.877	0.372	−2.337
7	0.980	0.386	−1.332
8	0.903	0.389	−1.716
9	1.065	0.358	−0.928
10	0.934	0.383	−1.312
11	0.894	0.385	−1.613
12	0.978	0.364	−1.001
13	0.972	0.349	−3.77
14	1.013	0.339	−4.049
15	0.989	0.403	−2.902
16	1.027	0.391	−3.107
17	0.978	0.428	−2.405
18	1.013	0.420	−2.574

This slow convergence can be essentially traced to the effect of numerous factors π^{2p}, $p=1,\ldots n/2$ appearing at perturbative orders g^n, g^{n+1} for $n\geq 2$ from the discontinuities. These terms clearly spoil the originally neat simple form of the large-N resummed mass in Eq. (4.2). Moreover, starting at order g^3 these π^{2p} terms come with larger coefficients *relative* to the other nonlogarithmic coefficients, originating from the $\ln m$ coefficients in the original perturbation (4.2) and (4.7) which are roughly all of the same order $\mathcal{O}(1)$. More precisely, by inspecting Eq. (4.7) one can see that at order g^2 the $-\pi^2/8$ contribution is (very roughly) numerically twice as large as the other nonlogarithmic coefficient $(1/2)$, while at order g^3 the relevant terms to be compared are the last two, $12/24$ and $-(13/24)\pi^2$, so the latter is an order of magnitude larger than the former. This explains the very good result at order g^2 and also the degraded result at the next g^3 order. A similar behavior is observed at higher orders, until at sufficiently high order the original perturbative coefficients of $\ln m$ also start to grow quickly, such that a balance with the π^{2p} contributions can again occur, with the (slow) convergence observed. Indeed, the spectral parameter optimization (3.16) tends to damp these relative π^{2p} contributions; for instance, the combined contributions of all L_λ-dependent terms for the optimal value $\tilde{L}_\lambda\sim -3.28$ at order g^3 in Table I almost cancel the large π^2 term. But since the latter terms are growing with the order, it is not surprising that the optimal $\tilde{L}_\lambda$ values are not very stable in Table I.

Interestingly, however, if instead of taking the exact results at a given order we consider a well-defined approximation, by keeping (at growing δ^n order) *only* π^{2p} terms with a fixed maximal power, then there is a higher δ^n order at which one recovers the simple exact RGOPT solution[6]: $\tilde{g}=1$, $\tilde{L}_\lambda=-1,\langle\bar{\Psi}\Psi\rangle_{\rm GN}=-\Lambda$. For instance, keeping only π^2 and π^4 terms (the latter appearing first at order g^4) and increasing the δ^k order, the exact solution is recovered at order δ^8. This cancellation mechanism thus indicates that the "maximal convergence"

[6]This nice property may appear somewhat artificial but it can be explained more rigorously. As observed in Ref. [20], the mass gap $M(m,g)$ at a given (sufficiently high) order δ^n has flat optima roughly at order $\sim n/2$ (i.e., its $n/2$th derivative with respect to m vanishes). Now for the spectral density, π^{2p} terms appearing at order g^p arise from Eq. (2.7) as the coefficient of the (logarithmic) derivatives $\partial/\partial\ln m$ of order p: so, *if* discarding terms of higher power $\pi^{2q}, q>p$, there is necessarily a fixed higher order at which the cancellation of all π^{2p} terms occurs.

properties of RGOPT (specific to the simpler GN model mass gap expression in Eq. (4.2) [20]) are not completely lost within the perturbative spectral density, but rather hidden, being obstructed by the more involved perturbative coefficients. These remarks are to be kept in mind when comparing with the QCD case below.

V. DETERMINATION OF THE QCD QUARK CONDENSATE

A. Perturbative three-loop quark condensate

The perturbative expansion of the QCD quark condensate for a nonzero quark mass can be calculated systematically from the related vacuum energy graphs. A few representative Feynman graph contributions at successive orders up to three-loop order are illustrated in Fig. 1 (there are evidently a few more three-loop contributions not shown here). Note that the one-loop order is $\mathcal{O}(1)=\mathcal{O}(g^0)$. The two-loop contributions were computed long ago [38] and the three-loop ones in Ref. [39]. Explicitly, the three-loop-order result in the $\overline{\rm MS}$ scheme reads

$$m\langle\bar{q}q\rangle_{\rm QCD}(m,g)=\frac{3}{2\pi^2}m^4\left(\frac{1}{2}-L_m+\frac{g}{\pi^2}\left(L_m^2-\frac{5}{6}L_m+\frac{5}{12}\right)+\left(\frac{g}{16\pi^2}\right)^2 q_3(m,n_f)\right), \tag{5.1}$$

where $m\equiv m(\mu)$ and $g\equiv 4\pi\alpha_S(\mu)$ are the running mass and coupling in the $\overline{\rm MS}$ scheme, and the three-loop coefficient reads[7] [39]

$$\begin{aligned}q_3(m,n_f)=&\frac{1}{27}(6185-768a_4-32\ln^4 2+192\ln^2 2\,z_2\\&+504z_3+(672z_3-750)n_f+528z_4)\\&+\left(52n_f-\frac{4406}{9}+\frac{32}{3}z_3\right)L_m\\&-\frac{32}{9}(5n_f-141)L_m^2+\frac{32}{9}(2n_f-81)L_m^3,\end{aligned} \tag{5.2}$$

where $z_i\equiv\zeta(i)$ and $a_4={\rm Li}_4(1/2)$.

The calculation in the dimensional regularization of Eq. (5.1) actually still contains divergent terms needing extra subtraction after mass and coupling renormalizations in the $\overline{\rm MS}$ scheme. The correct procedure to obtain an RG-invariant finite expression when subtracting those divergences consistently is well known in the standard renormalization of composite operators with mixing [40]. We can define [24] the needed subtraction as a perturbative series,

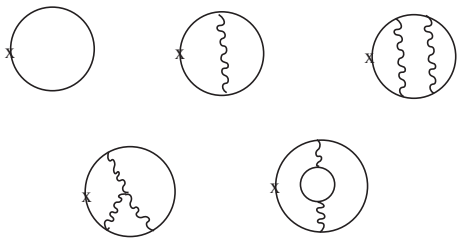

FIG. 1. Samples of standard perturbative QCD contributions to the chiral condensate up to three-loop order. The cross denotes a mass insertion.

$$\mathrm{sub}(g,m)\equiv\frac{m^4}{g}\sum_{i\geq 0}s_i g^i, \tag{5.3}$$

with coefficients determined order by order by

$$\begin{aligned}\mu\frac{\rm d}{{\rm d}\mu}\mathrm{sub}(g,m)&\equiv\mathrm{Remnant}(g,m)\\&=\mu\frac{\rm d}{{\rm d}\mu}[m\langle\bar{q}q\rangle(\mathrm{pert})|_{\rm finite}],\end{aligned} \tag{5.4}$$

where the remnant part is obtained by applying the RG operator (3.4) to the finite expression (5.1), which is not separately RG invariant. Equation (5.3) does not contain any $\ln m/\mu$ terms and necessarily starts with a s_0/g term to be consistent with RG invariance properties. To obtain RG invariance at order g^k [fixing s_k in Eq. (5.3)], one needs knowledge of the coefficient of the $\ln m$ term (equivalently the coefficient of $1/\epsilon$ in dimensional regularization) at order g^{k+1}. Concerning the condensate the extra contribution to the RG equation (5.4) is the so-called anomalous dimension of the QCD (quark) vacuum energy, which enters the renormalization procedure of the $m\langle\bar{q}q\rangle$ operator due to mixing with $m^4\times 1$ and is also given explicitly to three-loop order in Ref. [39]. The s_i coefficients can be expressed in terms of RG coefficients and other terms using RG properties. In compact form (for completeness in our normalization) they read[8]

[7]The originally calculated expressions in Ref. [39] are given for arbitrary N_c colors, n_h massive quarks, and n_l *massless* quarks entering at three-loop order. In our context m is the (n_f-degenerate) light-quark mass and its precise mass dependence is what is relevant for the optimization procedure, so one should trace properly the full n_l, n_h dependence, and take $n_l=0$, $n_h\equiv n_f$ with $n_f=2$ (3) for the SU(2) [SU(3)] case.

[8]The expression for s_3 (here approximated to 10^{-3} relative uncertainty, largely sufficient for our purpose) requires knowledge of the four-loop $\ln m/\mu$ coefficient, or alternatively the four-loop vacuum energy anomalous dimension. The latter, not explicitly available in the published literature so far, has been kindly provided to us by Chetyrkin and Maier [41] from a related work.

$$
\begin{aligned}
s_0 &= \frac{1}{4\pi^2(b_0-2\gamma_0)},\\
s_1 &= -\frac{1}{12\pi^2}+\frac{1}{4}\frac{b_1-2\gamma_1}{b_0-2\gamma_0},\\
s_2 &= -\frac{(112077+24519n_f+2101n_f^2+576(15-58n_f)z_3)}{1152\pi^4(-81+2n_f)(15+2n_f)},\\
s_3 &\simeq \frac{4.710^{-10}a_4(-81+2n_f)(-4.615+n_f)(15+2n_f)+2.47+1.275n_f+0.303n_f^2-0.019n_f^3+3.110^{-4}n_f^4}{(-57+2n_f)(-81+2n_f)(15+2n_f)}.
\end{aligned}
\tag{5.5}
$$

B. Perturbative spectral density

One crucial advantage of using the spectral density with the Banks-Casher relation (2.6) is that it gives direct access to the QCD condensate in the chiral limit, unlike the original direct RG-invariant expression $m\langle\bar{q}q\rangle$ in Eq. (5.1), where the condensate is screened by the mass for $m\to 0$. Indeed, note that a direct RGOPT optimization in the GN model of the corresponding expression $m\langle\bar{\Psi}\Psi\rangle$ gives an exactly vanishing result consistently at any order [22] (even though the optimized GN mass is clearly nonvanishing, $\tilde{m}=\Lambda$).

Thus, taking the logarithmic discontinuities according to Eqs. (2.7) and (3.9) gives us the perturbative spectral density up to three-loop order,

$$
-\rho_{\mathrm{QCD}}^{\overline{\mathrm{MS}}}(\lambda,g)=\frac{3}{2\pi^2}\lambda^3\left(-\frac{1}{2}+\frac{g}{\pi^2}\left(L_\lambda-\frac{5}{12}\right)+\left(\frac{g}{16\pi^2}\right)^2 q_3^{\mathrm{SD}}(\lambda,n_f)\right),
\tag{5.6}
$$

where now $L_\lambda\equiv\ln(|\lambda|/\mu)$ and

$$
q_3^{\mathrm{SD}}(\lambda,n_f)=\frac{1}{2}\left(52n_f-\frac{4406}{9}+\frac{32}{3}z_3\right)-\frac{32}{9}(5n_f-141)L_\lambda+\frac{32}{9}(2n_f-81)\left(\frac{3}{2}L_\lambda^2-\frac{\pi^2}{8}\right).
\tag{5.7}
$$

Note that the π^2 in the last term arises from the discontinuities of $\ln^3(m^2)$ according to Eq. (3.9). We now remark that none of the nonlogarithmic contributions in the *original* perturbative expression (5.1) contribute to the spectral density. Thus, similarly all subtraction terms in Eq. (5.5)—which are necessary for RG invariance of the original expression—do not contribute either, thus making the final expression to be optimized relatively simpler.

This point is worth elaborating in some detail. Just as for the GN model, instead of using the spectral density we could apply the RGOPT method more directly to the original perturbative expression of the condensate, Eq. (5.1), including in this case the subtractions (5.3) and (5.5) required by RG invariance [and also removing an overall factor m from Eq. (5.1) to define a nontrivial $\langle\bar{q}q\rangle$ in the chiral limit]. When this is done, one finds rather unstable values for the optimized mass, coupling, and resulting condensate, showing no clear empirical convergence pattern at successive orders, at least at the presently available (three-loop) order. Furthermore, these results tend to give a wrong-sign (positive, or ambiguous) condensate. More precisely, at the first nontrivial δ^0 (one-loop) order, there is no common nontrivial RG and OPT solution. Considering then the OPT or RG equations alone, both give a positive condensate, of roughly the right order of magnitude: $\langle\bar{q}q\rangle(\delta^0)=\sqrt{e}/(2\pi^2)\Lambda_{\overline{\mathrm{MS}}}^3\simeq 0.08\Lambda_{\overline{\mathrm{MS}}}^3$ from the OPT, and a very similar value is obtained from the RG. Next, at the δ^1 (two-loop) order, the (unique) AF-compatible branch solution of the combined RG and OPT equations (3.5) and (3.2) gives a complex-valued optimized coupling, mass, and condensate, with a negative real part for the condensate but a much larger imaginary part, $\langle\bar{q}q\rangle(\delta^1)\simeq(-0.08\pm 0.37i)\Lambda_{\overline{\mathrm{MS}}}^3$, a result that is clearly ambiguous. These calculations are also not very stable upon different truncations of perturbative higher-order terms in the RG equation (3.5). Furthermore, attempting to recover real AF-compatible solutions by a perturbative renormalization scheme change, both at orders δ and δ^2, happens to give no solutions (unlike for the pion decay constant case where the imaginary parts were small enough to allow for such a scheme change with very stable results [22]).

We can trace this wrong sign and unstable behavior to the fact that in four dimensions the (presumably dominant) one-loop contribution to the fermion condensate, given by the very first graph in Fig. 1, is quadratically divergent. The contribution of this quadratic divergence actually has the correct negative sign. Incidentally, in the Nambu–Jona-Lasinio model [4], an effective cutoff handles this divergence, and the quark condensate automatically has the correct sign. Note that in the NJL model the condensate (or equivalently the mass gap in the widely used leading-order large-N approximation) is precisely given by the very same first one-loop graph of Fig. 1, up to trivial overall factors, while genuine QCD contributions only enter at the next orders with gluon and further quark loop dressing. In

dimensional regularization, at lowest orders in the coupling, one finds that the extra subtractions (5.3) and (5.5) have a sign opposite to the sign of the similar terms in the GN model, and that this is due to the fact that the pole of $\Gamma(1-D/2)$ in the perturbative calculation of the condensate changes sign when going from dimension $D=2$ (corresponding to the logarithmic divergence in the GN model, and quadratic divergence in the $D=4$ NJL model) to dimension $D=4$ (corresponding to QCD). Indeed, as is well known most of the phenomenological successes of the NJL model rely strongly on the physical cutoff interpretation of the quadratically divergent mass gap in four dimensions.[9]

Hence, it appears that the RGOPT must lead to a wrong sign and/or unstable results, if applied directly to the QCD perturbative expression of the quark condensate evaluated in dimensional regularization and the related $\overline{\text{MS}}$ scheme at low orders. We do not know whether higher orders would cure this problem by ultimately stabilizing the result, but this appears rather unlikely since the first few orders are likely to remain dominant in our approach. (Indeed, a general property of the optimized perturbation is that the optimized coupling $\tilde{g}$ turns out to be reasonably small, so that the first few orders dominate.) We did not have this problem in our previous works [20–22] in which we were dealing with the pole mass and the pion decay constant, which are only logarithmically divergent quantities. Yet one should not hastily conclude that the OPT or RGOPT approaches are bound to fail in any situation where quadratic divergences would be present in a cutoff regularization.[10] Rather, the above problems stress that in a given model it is crucial to choose carefully the basic entity to be perturbatively modified and optimized within the RGOPT framework. (This is analogous to the traditional variational Rayleigh-Ritz method in quantum mechanics, where the trial wave functions should often be appropriately chosen to obtain a sensible result.) This is why for QCD one must use instead the spectral density, which in our framework we anyway derived from the very same original perturbative condensate expression (5.1), but which at the same time formally gets rid of the influence of quadratic divergences. Indeed, only the infrared part $\lambda \to 0$ in Eq. (2.5) can generate a nonzero result in the chiral limit, which is thus insensitive to ultraviolet divergences [16]. We note also that lattice evaluations of the condensate also bypass this potential quadratic divergence problem by using the spectral density [12,13], or by extracting the condensate by more indirect methods, e.g., by relying on the GMOR relation.

We thus proceed with the actual RGOPT calculations for the spectral density at successive perturbative orders. First we remark that, since there is no logarithmic L_λ contribution in the spectral density at one-loop order [the one-loop $\ln m$ contribution in Eq. (3.10) only gives the constant $1/2$], there is no nontrivial $\lambda \neq 0$ optimized solution of Eq. (3.16) at one-loop order. Thus we should start applying our method at the next two-loop order.

C. Two-loop $\mathcal{O}(\delta)$ results

Let us perform step by step the RGOPT optimization by first restricting Eq. (5.6) at the first nontrivial two-loop order. Concerning the δ expansion given by Eq. (3.14), it is crucial [21,22] to take the right value of the exponent a, determined by the lowest-order anomalous mass dimension, which makes the δ-modified series match AF and compatible with RG properties, as we recalled in some detail in Sec. III B. In the case of the large-N limit of the GN model, one has simply $a=\gamma_0/(2b_0)=1$. Actually, since $m\langle\bar{q}q\rangle$ is RG invariant to all orders rather than $\langle\bar{q}q\rangle$, it is easily derived that the correct value to be used for $\langle\bar{q}q\rangle$, and thus for the related spectral density from Eq. (2.5), is

$$a=\frac{4}{3}\left(\frac{\gamma_0}{2b_0}\right). \tag{5.8}$$

Then to first nontrivial order in δ the modified series reads

$$-\rho^{\delta^1}_{\text{QCD}}=\frac{3}{2\pi^2}\lambda^3\left(\frac{19}{58}+\frac{g}{\pi^2}\left(L_\lambda-\frac{5}{12}\right)\right), \tag{5.9}$$

and the OPT (3.16) and RG (3.13) equations have a unique solution [using also Eq. (2.6)], given in the first line of Table II. For a simpler first illustration we actually used the RG equation (3.13) at the very first order with the one-loop coefficient b_0, in order to get simple analytic solutions. Therefore we obtain $\langle\bar{q}q\rangle^{1/3}(n_f=2)(\mu\simeq 2.2\bar{\Lambda}_2)\simeq -0.96\bar{\Lambda}_2$, a fairly decent value given this lowest nontrivial order. At two-loop perturbative order Eq. (5.9) does not depend explicitly on the number of flavors n_f, but an n_f dependence enters into the optimized results indirectly from the RG equation (3.13) involving $b_0(n_f)$, which also enters $\bar{\Lambda}_{n_f}$. The corresponding optimized coupling is $\tilde{\alpha}_S \equiv \tilde{g}/(4\pi)\simeq 0.83$, a moderately large value very similar to the optimal coupling values obtained, at first nontrivial RGOPT order, when considering the pion decay constant F_π in Ref. [22]. Of course the precise number obtained for the condensate depends on the precise definition of the $\bar{\Lambda}$ reference scale, which is generally perturbative and a matter of convention. To get the numbers in the first lines of Table II we have used the simpler one-loop form, $\bar{\Lambda}=\mu e^{-1/(2b_0 g)}$, consistently with the one-loop RG

[9]The NJL model may be formulated in dimensional regularization to some extent, in dimensions $2<D<4$, but with rather odd properties; see, e.g., Ref. [42].

[10]In fact the (standard) OPT has been applied in the framework of the effective NJL model with a cutoff at next-to-leading δ order [33], giving sensible results beyond the large-N approximation, and consistent with important basic properties like the Goldstone theorem, the GMOR relation, etc.

TABLE II. Main optimized results at successive orders for $n_f = 2$, for the optimized spectral parameter $\tilde{\lambda}$, the optimized coupling $\tilde{\alpha}_S$, and the resulting optimized condensate. We also give the RG-invariant condensate $\langle\bar{q}q\rangle^{1/3}_{\rm RGI}$ calculated at the consistent perturbative order from Eq. (5.10). $\bar{\Lambda}_2$ is conventionally normalized everywhere by Eq. (5.11), except in the very first line where the one-loop expression $\bar{\Lambda} \equiv \mu e^{-1/(2b_0 g)}$ is used.

δ^k, RG order	$\ln\frac{\tilde{\lambda}}{\mu}$	$\tilde{\alpha}_S$	$\frac{-\langle\bar{q}q\rangle^{1/3}}{\bar{\Lambda}_2}(\tilde{\mu})$	$\frac{\tilde{\mu}}{\bar{\Lambda}_2}$	$\frac{-\langle\bar{q}q\rangle^{1/3}_{\rm RGI}}{\bar{\Lambda}_2}$
δ, RG one-loop	$-\frac{2275}{10092}$	$\frac{87\pi}{328} \simeq 0.83$	0.962	2.2	0.996
δ, RG two-loop	−0.45	0.480	0.822	2.8	0.821
δ^2, RG two-loop	−0.686	0.483	0.792	2.797	0.792
δ^2, RG three-loop	−0.703	0.430	0.794	3.104	0.783
δ^3, RG three-loop	−0.838	0.405	0.793	3.306	0.774
δ^3, RG four-loop	−0.820	0.391	0.796	3.446	0.773

equation used. When making precise comparisons with other phenomenological determinations of the condensate, we will use a more precise perturbative definition of $\bar{\Lambda}$ at four-loop order, in agreement with most other present determinations. We also remark that because the condensate is scale dependent our RGOPT optimization also fixes a scale, consistently with a defining convention for $\bar{\Lambda}$, as indicated in Table II.

For $n_f = 3$ at order δ one finds similarly the optimized results given in the first line of Table III, which are indeed very close to the $n_f = 2$ results above.

Now, since our basic expression originated from an exact two-loop calculation, it is *a priori* more sensible to apply the RG equation (3.13) at the same two-loop order, in order to capture higher-order effects as much as possible. Doing this, we obtain the results given in the second lines of Tables II and III for $n_f = 2, 3$. These results should therefore be considered more consistent at two-loop order. One can already observe the substantial decrease of the optimal coupling α_S to a more perturbative value, and the correspondingly higher optimal scale μ, with respect to the results using the pure one-loop RG equation.

For completeness and later use we also give in Tables II and III the corresponding values of the *RG-invariant* condensate $\langle\bar{q}q\rangle_{\rm RGI}$, perturbatively defined in our normalization as

$$\langle\bar{q}q\rangle_{\rm RGI} = \langle\bar{q}q\rangle(\mu)(2b_0 g)^{\frac{\gamma_0}{2b_0}}\left(1+\left(\frac{\gamma_1}{2b_0}-\frac{\gamma_0 b_1}{2b_0^2}\right)g+\mathcal{O}(g^2)\right), \tag{5.10}$$

where higher-order terms not shown here are easily derived from integrating $\exp\left[\int dg\gamma_m(g)/\beta(g)\right]$, which are known perturbatively to four-loop g^3 order since they only depend on the RG function coefficients [34] b_i, γ_i. The factor multiplying the scale-dependent condensate $\langle\bar{q}q\rangle(\mu)$ in Eq. (5.10) is obviously the inverse of the one defining similarly a scale-invariant mass, given explicitly to four-loop order in the literature (see, e.g., Ref. [43]). We will calculate the RG-invariant condensate at successive orders in Tables II and III using Eq. (5.10) consistently at the same perturbative order as the RG order used in Eq. (3.13), and taking $g \equiv \tilde{g} = 4\pi\tilde{\alpha}_S$, the corresponding optimized values obtained at each order. [Alternatively, we could directly optimize Eq. (5.10) instead of $\langle\bar{q}q\rangle(\mu)$, with the last term $\propto \gamma_m(g)$ in the RG equation (3.13) removed. This gives the same optimized solutions (as expected since it is formally completely equivalent) up to tiny numerical differences due to perturbative reexpansions, of less than 10^{-3} relative to the numbers given in Tables II and III.]

D. Three-loop $\mathcal{O}(\delta^2)$ results

At three-loop g^2 order the n_f dependence enters explicitly within the perturbative expression of the spectral density; see Fig. 1 and the last g^2 coefficient in Eqs. (5.6) and (5.7). This is also interesting in view of other results on the variation of the condensate value with the number of flavors [2,18].

We find a unique real AF-compatible optimized solution. More precisely, at this three-loop order there are actually two real optimized solutions for $\tilde{L}_\lambda$, $\tilde{\alpha}_S$, but the selection of the right physical solution is unambiguous since only one is clearly compatible with AF behavior for $g = 4\pi\alpha_S \to 0$, $\ln(\tilde{\lambda}/\mu) \simeq -d_k/(2b_0 g) + \mathcal{O}(1)$ with $d_k = \mathcal{O}(1)$, both for the RG and OPT equations.[11] In contrast, the other real solution has for $g \to 0$ a coefficient of opposite sign to AF and gives $\tilde{L}_\Lambda = \ln\tilde{\lambda}/\mu > 0$, which also implies incompatibility with perturbativity since we expect $\mu \gg \tilde{\lambda}$, just like the perturbative range $\mu \gg \tilde{m} \sim \bar{\Lambda}$ for the original expansion with mass dependence. Explicitly, we obtain for $n_f = 2, 3$ the results given in the third and fourth lines of Tables II and III, respectively. More precisely, as indicated

TABLE III. Same as Table II for $n_f = 3$.

δ^k order	$\ln\frac{\tilde{\lambda}}{\mu}$	$\tilde{\alpha}_S$	$\frac{-\langle\bar{q}q\rangle^{1/3}}{\bar{\Lambda}_3}(\tilde{\mu})$	$\frac{\tilde{\mu}}{\bar{\Lambda}_3}$	$\frac{-\langle\bar{q}q\rangle^{1/3}_{\rm RGI}}{\bar{\Lambda}_3}$
δ, RG one-loop	$-\frac{283}{972}$	$\frac{27\pi}{104} \simeq 0.82$	0.965	2.35	0.987
δ, RG two-loop	−0.56	0.474	0.799	3.06	0.789
δ^2, RG two-loop	−0.766	0.493	0.776	2.942	0.772
δ^2, RG three-loop	−0.788	0.444	0.780	3.273	0.766
δ^3, RG three-loop	−0.967	0.414	0.769	3.540	0.745
δ^3, RG four-loop	−0.958	0.400	0.773	3.700	0.744

[11] Due to the nontrivial relations between $\ln m$ and $\ln\lambda$, Eqs. (3.9) and (3.10), the $1/g$ coefficient of the correct AF branch $L_\lambda(g)$ for $g \to 0$ is not exactly $-1/(2b_0)$, like it is for $\ln m/\mu$ [Eq. (3.6)], which is essentially determined by the leading logarithms' $g^k \ln^k(m/\mu)$ behavior. But this $1/g$ coefficient has the correct AF sign, being at order δ^k: $-d_k/(2b_0)$ with $d_k > 0$ a constant close to 1, which slowly approaches $d_k \to 1$ as the perturbative order k increases.

there the results in the third line were obtained by taking the RG equation (3.13) truncated at two-loop order, while the results in the fourth line were obtained by taking the full three-loop RG equation. These results exhibit a very good stability when confronted with the relative arbitrariness in the order of the RG equation. Of course it is more legitimate to use the three-loop RG equation consistently at this three-loop order, which we shall adopt for our final determination of the condensate. Notice also that the optimal values $\tilde{\alpha}_S$ decreased by almost a factor os 2 with respect to the lowest nontrivial order result above, which indicates that the resulting series is much more perturbative. But $\tilde{\alpha}_S$ almost does not change as compared to the more consistent two-loop results. Similarly, $\tilde{\alpha}_S$ further slightly decreases and the optimal scale $\tilde{\mu}$ increases when going from two to three loops in the RG equation (3.13).

As a matter of numerical detail, to obtain the results in Tables II and III we took the convention of the QCD scale $\bar{\Lambda}$ based on a perturbative four-loop expression [44]:

$$\bar{\Lambda}^{4-\text{loop}}_{n_f}(g) \equiv \mu e^{-\frac{1}{2b_0 g}}(b_0 g)^{-\frac{b_1}{2b_0^2}} \exp\left[-\frac{g}{2b_0}\cdot\left(\left(\frac{b_2}{b_0}-\frac{b_1^2}{b_0^2}\right)+\left(\frac{b_1^3}{2b_0^3}-\frac{b_1 b_2}{b_0^2}+\frac{b_3}{2b_0}\right)g\right)\right]. \quad (5.11)$$

This is convenient and important for making precise comparisons with most recent determinations, using the same four-loop perturbative order conventions for $\bar{\Lambda}$. Actually, when using the RG equation (3.13) at order δ^k it would be more natural to adopt a $\bar{\Lambda}$ convention at the consistent $(k+1)$-loop order $\bar{\Lambda}_{k+1}$ [given by Eq. (5.11)] by taking $b_3 = 0$ (and $b_2 = 0$) at three loops (two loops). But this only affects an overall normalization of the final result, as $\bar{\Lambda}$ itself is not involved in the actual optimization process when using Eqs. (3.2) and (3.13). Besides, starting at three-loop order the differences obtained from such different conventions are minor. (The $\bar{\Lambda}$ convention also affects the precise value of the optimal scales $\tilde{\mu}/\bar{\Lambda}$ in Tables II and III, from which we shall start the evolution to a higher scale to compare with other determinations in the literature; see below.) Strictly speaking, the different values of $\langle\bar{q}q\rangle(\mu)$ obtained in Tables II and III, e.g., at three-loop order cannot be directly compared, as they are obtained at different scales $\tilde{\mu}$. Thus we also give the scale-invariant condensate values $\langle\bar{q}q\rangle_{\text{RGI}}$ which can be more appropriately compared.

Notice also that in spite of the more than 10% change in the optimal coupling $\tilde{\alpha}_S$ when taking two- or three-loop RG, the final physical value of the condensate only varies by 0.25%[12]: this also reflects a strong stability. Moreover, the value of $\langle\bar{q}q\rangle^{1/3}/\bar{\Lambda}$ changes by about 20% with respect to the crude two-loop-order result (first lines of Tables), but it changes by much less when compared to the more consistent two-loop-order result (second lines). This shows *a posteriori* that stability appears at the first nontrivial two-loop result, with an already quite realistic value. This stability—which suggests that we remain within the domain of validity of perturbation theory—is an important requirement for the usefulness of our method. A similar behavior was observed when optimizing the pion decay constant in Ref. [22]. We also note that the optimized coupling values $\tilde{\alpha}_S$ at successive orders happen to be rather close to those for which the scale invariance factor in Eq. (5.10) multiplying $\langle\bar{q}q\rangle(\mu)$ would be exactly one (which for $n_f = 2$ happens for $\alpha_S \simeq 0.483$, 0.461, 0.457 at two-, three-, and four-loop order, respectively). In other words, $\tilde{\alpha}_S$ is close to a (variational) "fixed-point" scale-invariant behavior. Had we found optimized $\tilde{\alpha}_S$ values that were a factor of 2–3 smaller or larger, we would obtain no valuable results beyond ordinary perturbation in the first case, or much more unstable results in the second case. However, we stress that the optimal coupling $\tilde{\alpha}_S$ or optimal mass $\tilde{m}$ do not really have a universal physical interpretation since the precise $\tilde{\alpha}_S$ and $\tilde{m}$ values depend on the physical quantity being optimized. For instance, when optimizing F_π in Ref. [22] at a given perturbative order, the corresponding $\tilde{\alpha}_S$ values were pretty close to the present ones, but nevertheless slightly different. The physically meaningful result is obtained when replacing $\tilde{\alpha}_S$ and $\tilde{\lambda}$ within the quantity being optimized, like the condensate studied here.

Comparing Tables II and III, it is also clear that the *ratio* of the quark condensate to $\bar{\Lambda}^3$ has a moderate dependence on the number of flavors n_f, although there is a definite trend that $\langle\bar{q}q\rangle^{1/3}_{n_f=3}$ is smaller by about 2–3% with respect to $\langle\bar{q}q\rangle^{1/3}_{n_f=2}$ (in units of $\bar{\Lambda}_{n_f}$) at the same perturbative orders. The smallness of this difference was quite expected, due to the n_f dependence only appearing at three-loop order and the overall stability of the modified perturbation. However, from various different estimations, including lattice [45] and ours [22], there are some indications that $\bar{\Lambda}_2 > \bar{\Lambda}_3$ (although unclear from uncertainties, due to a larger uncertainty on $\bar{\Lambda}_2$), which therefore could indirectly further affect the actual flavor dependence of the condensate. We shall come back to this point in more detail in the phenomenological discussion in the next section, after establishing our final result for the precise condensate values.

E. Four-loop $\mathcal{O}(\delta^3)$ results

We finally consider the optimization of the spectral density at four-loop order, the maximal order available at present. In fact, the complete standard perturbative

[12]This result appears to be so stable partly due to the $1/3$ power of the condensate in Tables II and III. For the actual optimization performed on the quantity $\langle\bar{q}q\rangle$, the corresponding variation is $\simeq$0.7%.

expression of our starting expression for the condensate, i.e., the next α_S^3-order correction to Eq. (5.1), is not fully known at present. But it obviously takes the form

$$m\langle\bar{q}q\rangle_{\rm QCD}^{4-\rm loop}(m,g) = \frac{3}{2\pi^2}m^4\left(\frac{g}{16\pi^2}\right)^3(c_{40}L_m^4+c_{41}L_m^3+c_{42}L_m^2+c_{43}L_m+c_{44}), \tag{5.12}$$

where $L_m \equiv \ln(m/\mu)$ and we choose a convenient overall normalization with respect to the lowest-order terms in Eq. (5.1). Now the leading, next-to-leading, and next-to-next-to-leading logarithm coefficients c_{40}–c_{42} are easy to derive from RG invariance properties, as they are fully determined by lowest orders. The next-to-next-to-next-to-leading logarithm $\ln m$ coefficient c_{43} can also be inferred by RG properties from the available anomalous dimension of the vacuum energy, calculated by Chetyrkin and Maier [41], and related to s_3 given in Eq. (5.5). Explicitly, we obtain

$$\begin{aligned} c_{40} &\simeq 4836.74(4533.33),\\ c_{41} &\simeq -12282.5(-11292.4),\\ c_{42} &\simeq 15606.4(12648.1),\\ c_{43} &\simeq -18588.6(-15993.5), \end{aligned} \tag{5.13}$$

where the first and second numbers correspond to $n_f = 2$ and $n_f = 3$, respectively. [N. B.: We can obtain the generic algebraic values of $c_{4i}(n_f)$ but these are rather involved and not particularly instructive, so we prefer to keep an approximate numerical form for the relevant $n_f = 2$, 3 case in Eq. (5.13).] Thus only the nonlogarithmic coefficient c_{44} is actually unknown at present, and it could be quite challenging to compute. But since the nonlogarithmic parts cannot contribute to the spectral density, the latter can thus be fully determined at four loops! This gives for the *exact* perturbative four-loop contribution to the spectral density, after taking the logarithmic singularities according to Eqs. (2.7) and (3.9),

$$-\rho_{\text{4-loop}}^{\overline{\rm MS}}(\lambda) = \frac{3}{2\pi^2}\lambda^3\left(\frac{g}{16\pi^2}\right)^3\left(c_{40}(n_f)\left(2L_\lambda^3-\frac{\pi^2}{2}L_\lambda\right) + c_{41}(n_f)\left(\frac{3}{2}L_\lambda^2-\frac{\pi^2}{8}\right)+c_{42}(n_f)L_\lambda + \frac{1}{2}c_{43}(n_f)\right), \tag{5.14}$$

which should be added to the three-loop expression in Eq. (5.6). It allows us to calculate the spectral density and the related condensate at three successive orders of the variationally modified perturbation, which gives further confidence and an important stability and convergence check of our result.

We obtain at four-loop order once more a unique real common RG and OPT AF-compatible solution. (The brute optimization results actually give several real solutions for $\tilde{\lambda}$, $\tilde{\alpha}_S$ but there are no possible ambiguities since all solutions are eliminated from the AF compatibility requirement, except a single one, with $\tilde{\alpha}_S > 0$ and $\tilde{L}_\lambda < 0$ as expected.) Explicitly, we obtain the optimization results given in the fifth and sixth lines of Tables II and III for $n_f = 2$, 3, respectively, where to illustrate the stability the fifth lines correspond to taking the RG equation (3.13) at three-loop order, and the sixth lines (more consistently) at four-loop order [with $\bar{\Lambda}$ now always being taken at four-loop order from Eq. (5.11)]. One observes a further decrease of the optimal coupling $\tilde{\alpha}_S$ to more perturbative values, with respect to the three-loop results above, as well as the corresponding decrease of $\tilde{L}_\lambda$, meaning that $\tilde{\mu}$ is also larger. The stabilization/convergence of the results is even clearer for the scale-invariant condensate $\langle\bar{q}q\rangle_{\rm RGI}$ given in the last columns in Tables II and III, which at four-loop order has almost no variation upon RG equation truncations.

To better appreciate the very good stability of these results, consider the basic perturbative expression of the condensate (5.6) up to four loops in a more numerical form (for $n_f = 2$) and a more standard normalization of the coupling:

$$\begin{aligned} -\rho_{\rm QCD}^{\overline{\rm MS}}&(4-\text{loop})(\lambda)\\ &\simeq \frac{3}{2\pi^2}\lambda^3\left(-\frac{1}{2}+\frac{4\alpha_S}{\pi}(L_\lambda-0.42)\right.\\ &\quad\left.+\left(\frac{\alpha_S}{\pi}\right)^2(9.46+(29.1-25.7L_\lambda)L_\lambda\right)\\ &\quad+\left(\frac{\alpha_S}{\pi}\right)^3(91.5+L_\lambda(-129+L_\lambda(-288+151L_\lambda))). \end{aligned} \tag{5.15}$$

From this one can easily appreciate that the successive perturbative terms are not small, just like in most perturbative QCD series: at successive orders the coefficients grow rapidly (even if partly damped by the decreasing α_S/π higher powers, provided that α_S remains rather moderate). In fact, for the relevant values of $\tilde{\alpha}_S \simeq 0.4$–$0.5$ and typically $\tilde{L}_\lambda \simeq -(.7$–$.8)$ (depending on the RGOPT order), all successive perturbative terms are roughly of the same order of magnitude. Now for the variationally modified perturbation the successive sequences are quite different, but before any optimization the resulting series in α_S has perturbative coefficients that similarly grow at successive orders. But the RGOPT mass and coupling optimization manage to stabilize the series in such a way that the discrepancies between the three- and four-loop orders in the final $\langle\bar{q}q\rangle^{1/3}$ results are about 2% or less. Thus it is

important that the optimized sequence has clearly further stabilized from three- to four-loop order, to be more confident in a precise determination of the condensate, although the variation from the lowest nontrivial two-loop to three-loop results (∼4%) was already very reasonable.

It appears that these QCD RGOPT results are more stable than the corresponding ones for the spectral density of the yet simpler large-N GN model in Table I. This is a bit surprising *a priori*, given that direct optimizations (not going through the spectral density) give maximal convergence for the large-N GN model [20]. In fact one can understand these results as follows. As explained in Sec. IV, the rather slow convergence for the GN spectral density is entirely due to the large and growing factors of π^{2p} coming from the discontinuities (3.9) at successive orders, which spoil the simple form of the series and "screen" the otherwise maximal convergence with the neat solution (4.6). Now although the π^{2p} coefficients from Eq. (3.9) are universal (and thus the same for QCD), once combined with the original perturbative coefficients of Eq. (5.1) their *relative* contributions with respect to the other perturbative terms remain more reasonably of the same order in the QCD case than in the GN case. This is because the original perturbative coefficients are comparatively larger in the QCD case. More precisely, by inspecting the QCD spectral density series at three-loop order g^2 in Eq. (5.7), we see that the π^2 contribution [last term on the rhs of Eq. (5.7)] is roughly twice the other nonlogarithmic contribution [first term on the rhs of Eq. (5.7)]. Similarly, at the next four-loop g^3 order from Eq. (5.12) the π^2 contributions are roughly twice the other nonlogarithmic contribution ($c_{43}/2$). As long as those π^{2p} contributions remain roughly of the same order of magnitude as the original perturbative coefficients, such that some balance can occur from the optimization process, they should produce a moderate disturbance of the observed stability. We expect these properties to remain true at even higher orders, because the original QCD perturbation coefficients also grow rapidly with the order.

The fourth and sixth lines of Tables II and III give our direct optimization results for $n_f = 2, 3$ and three or four loops, respectively. To get a final result it could be legitimate to take only the presumably more precise maximal four-loop perturbative order available, as is commonly done in most perturbative analyses. However, to allow for a more realistic estimate of the theoretical error of our results, we will more conservatively consider the difference between the three- and four-loop results (but using a consistent RG perturbative order in each case) as defining the theoretical uncertainty.

VI. EVOLUTION TO HIGHER ENERGY AND PHENOMENOLOGICAL COMPARISON

In order to get a more precise result it is necessary to take into account the (moderate but not completely negligible) running of the condensate values, since the optimal scales obtained are somewhat different at three- and four-loop order, though they are reasonably perturbative (roughly of order $\tilde{\mu} \gtrsim 1$ GeV). It is necessary to perform a further evolution of the scale if only to make contact with the more standard scale $\mu \simeq 2$ GeV where other (sum rules, lattice, etc.) condensate determinations are often conventionally given.

A. RGOPT $\langle\bar{q}q\rangle(\mu = 2\ \mathrm{GeV})$ results for $n_f = 2$ and $n_f = 3$

The procedure to perturbatively evolve the condensate from one scale to another is straightforward since from the exact RG invariance of $m\langle\bar{q}q\rangle$ it is simply given by the inverse of the well-known running of the quark masses,

$$\langle\bar{q}q\rangle(\mu') = \langle\bar{q}q\rangle(\mu)\exp\left[\int_{g(\mu)}^{g(\mu')} dg\frac{\gamma_m(g)}{\beta(g)}\right]. \quad (6.1)$$

Alternatively, we may take the values of the scale-invariant condensate (5.10) as obtained in the last columns of Tables II and III and extract from those the condensate at any chosen (perturbative) scale μ' by using Eq. (5.10) again, but now taking $g \equiv 4\pi\alpha_S(\mu')$. This is of course fully equivalent to performing the running from μ to μ' with Eq. (6.1). Since all relevant scales $\tilde{\mu}$ obtained above are in a fairly perturbative range $\gtrsim$1 GeV, we take a (four-loop) perturbative evolution.[13] We choose the highest optimized scales obtained (given by the four-loop results for both the $n_f = 2$ and $n_f = 3$ cases) as the reference low scale(s): $\mu_{\mathrm{ref}}(2) = 3.45\bar{\Lambda}_2$ and $\mu_{\mathrm{ref}}(3) = 3.70\bar{\Lambda}_3$, respectively. (N. B.: Given the present values of $\bar{\Lambda}_3 \simeq 340 \pm 8$ MeV [44], $\mu_{\mathrm{ref}}(3)$ happens quite accidentally to be just below the charm-quark mass threshold). For example, this running gives a ≃2% increase of the three-loop $\langle\bar{q}q\rangle^{1/3}_{n_f=2}$ value given in Table II and quite similarly for $n_f = 3$. Putting all this together, we obtain

$$-\langle\bar{q}q\rangle^{1/3}_{n_f=2}(\mu_{\mathrm{ref}}(2) = 3.45\bar{\Lambda}_2) = (0.796 - 0.808)\bar{\Lambda}_2,$$
$$-\langle\bar{q}q\rangle^{1/3}_{n_f=3}(\mu_{\mathrm{ref}}(3) = 3.70\bar{\Lambda}_3) = (0.773 - 0.796)\bar{\Lambda}_3, \quad (6.2)$$

which are our intermediate results in terms of $\bar{\Lambda}$ and at the respective $n_f = 2, 3$ optimal scales, including our estimated theoretical uncertainties (roughly of order 2%) given by the range of differences between the three-loop results

[13]For $n_f = 2$, it is implicitly understood that this evolution is performed in a simplified QCD world where the strange and heavier quarks are all infinitely massive, i.e., "integrated out." Otherwise it would not make sense perturbatively to take into account the strange-quark mass threshold effects on the running. For $n_f = 3$ we can perform a more realistic running, properly taking into account the charm-quark mass threshold effects on $\alpha_S(\mu \sim m_c)$; see below.

(evolved to the scales $\mu_{\rm ref}$) and direct four-loop results. We give results in the form of Eq. (6.2) in view of possibly more precise determinations of $\bar{\Lambda}_{2,3}$ in the future. Note that for both $n_f = 2, 3$ the lowest values given in Eq. (6.2) correspond to the presumably more accurate maximal four-loop results, which gave the $\mu_{\rm ref}$ values directly from optimization, and thus without possible extra uncertainties from running.

Next we perform a final evolution from the low reference scales $\mu_{\rm ref}(2, 3)$ relevant for $n_f = 2$ and $n_f = 3$, respectively [as given in Eq. (6.2)], up to the conventional scale $\mu' = 2$ GeV, where from the present world average for $\bar{\Lambda}_3$ we find $\bar{\alpha}_S(2\ \text{GeV}) \simeq 0.305 \pm 0.004$. For $n_f = 3$ we take into account the four-loop expression of the perturbative matching [46] at the crossing of the charm-quark threshold. Overall this leads to an increase of the values in Eq. (6.2) for $|\langle\bar{q}q\rangle|^{1/3}$ of about ∼4.6% for $n_f = 2$ and 5.3% for $n_f = 3$ [in which we take into account the charm-quark threshold with matching relations for $\alpha_S(\mu \simeq m_c)$, which contributes up to $\sim -0.3\%$ with respect to a more naive one-step evolution ignoring charm-threshold effects]. More precisely,

$$-\langle\bar{q}q\rangle^{1/3}_{n_f=2}(2\ \text{GeV}) = (0.833 - 0.845)\bar{\Lambda}_2,$$
$$-\langle\bar{q}q\rangle^{1/3}_{n_f=3}(2\ \text{GeV}) = (0.814 - 0.838)\bar{\Lambda}_3. \quad (6.3)$$

To give a more precise determination for $n_f = 2$ one obstacle is the presently not very precisely known value of the basic scale $\bar{\Lambda}_2$. In principle it is beyond the reach of the purely perturbative approach, as it cannot be "perturbatively connected" to the more precisely known $\bar{\Lambda}_3$ value [44]. Our own estimate [22] of $\bar{\Lambda}_2$ from the pion decay constant gave $\bar{\Lambda}_2 \simeq 360^{+42}_{-30}$ MeV, while some recent lattice determinations are $\bar{\Lambda}_2 \simeq 330 \pm 45$ (staggered Wilson fermions [45]) and $\bar{\Lambda}_2 \simeq 331 \pm 21$ (quark static potential method [47]). (Incidentally, this latter precise lattice determination tended to increase the central value of $\bar{\Lambda}_2$ by ∼15 GeV with respect to previous similar determinations [48]). Since lattice uncertainties are mostly statistical and systematic (while ours are theoretical errors), it is not obvious how to combine all of these in a sensible manner. We thus prefer to keep separate estimates. For a representative illustration, combining our present results in Eq. (6.3) with the above-quoted most precise lattice values of $\bar{\Lambda}_2$, we obtain

$$-\langle\bar{q}q\rangle^{1/3}_{n_f=2}(2\,\text{GeV}, \text{lattice}\,\bar{\Lambda}_2) \simeq 278 \pm 2 \pm 18\,\text{MeV}, \quad (6.4)$$

where the first quoted error is our intrinsical theoretical error propagated from the one in Eq. (6.2), while the second larger uncertainty originates from the lattice ones on $\bar{\Lambda}_2$. Using instead only our above-quoted RGOPT determination [22] of $\bar{\Lambda}_2$ gives somewhat higher values with larger uncertainties:

$$-\langle\bar{q}q\rangle^{1/3}_{n_f=2}(2\ \text{GeV}, \text{rgopt}\,\bar{\Lambda}_2) \simeq 301 \pm 2^{+35}_{-25}\ \text{MeV}. \quad (6.5)$$

For $n_f = 3$ the more precisely known $\bar{\Lambda}_3$ value from many different determinations allows for a more precise determination of the condensate. Taking the latest world average values [44] $\bar{\alpha}_S(m_Z) = 0.1185 \pm 0.0006$, which translates to $\bar{\Lambda}_3^{wa} = 340 \pm 8$ MeV, we obtain

$$-\langle\bar{q}q\rangle^{1/3}_{n_f=3}(2\ \text{GeV}, \bar{\Lambda}_3^{\rm wa}) \simeq 281 \pm 4 \pm 7\ \text{MeV}, \quad (6.6)$$

where again the first error is our estimated theoretical uncertainty and the second one is from the world-averaged $\bar{\Lambda}_3$. Using instead only our RGOPT determination [22] of $\bar{\Lambda}_3 = 317^{+27}_{-20}$ MeV gives slightly lower values, but with larger uncertainties:

$$-\langle\bar{q}q\rangle^{1/3}_{n_f=3}(2\ \text{GeV}, \text{rgopt}\,\bar{\Lambda}_3) \simeq 262 \pm 4^{+22}_{-17}\ \text{MeV}. \quad (6.7)$$

Finally, rather than fixing the scale from $\bar{\Lambda}$, it may be more sensible to give our results for the ratio of the scale-invariant condensate with another physical scale, which is a parameter-free prediction. Taking the $\langle\bar{q}q\rangle^{1/3}_{\rm RGI}$ results in Tables II and III and using only our previous RGOPT results [22] for $F/\bar{\Lambda}_2$ and $F_0/\bar{\Lambda}_3$ [where F and F_0 are the pion decay constants for $n_f = 2$, $n_f = 3$, respectively, in the chiral limit], we obtain

$$\frac{-\langle\bar{q}q\rangle^{1/3}_{\text{RGI},n_f=2}}{F} = 3.25 \pm 0.02^{+0.35}_{-0.24}, \quad (6.8)$$

where the first error comes from the present calculation of the condensate, while the second one comes from taking the most conservative range linearly combining three- and four-loop-order uncertainty results for $F/\bar{\Lambda}_2$ from Eq. (4.28) of Ref. [22]. A less conservative estimate may be obtained alternatively by taking the range spanned by the maximal available four-loop results for $F/\bar{\Lambda}_2$ correlated with the four-loop condensate results. This gives

$$\frac{-\langle\bar{q}q\rangle^{1/3}_{\text{RGI},n_f=2}}{F} = 3.26 \pm 0.01^{+0.22}_{-0.16}. \quad (6.9)$$

Similarly, for $n_f = 3$ we obtain

$$\frac{-\langle\bar{q}q\rangle^{1/3}_{\text{RGI},n_f=3}}{F_0} = 3.04 \pm 0.04^{+0.14}_{-0.07}, \quad (6.10)$$

where the first theoretical error comes from the condensate, while the second one comes from the conservative range

linearly combining three- and four-loop-order uncertainty results on $F_0/\bar{\Lambda}_3$ from Eq. (4.30) of Ref. [22]. As observed above, the direct results from the optimization of $-\langle\bar{q}q\rangle(n_f)/\bar{\Lambda}^3_{n_f}$ in Tables II and III show a moderate relative decrease of about 2–3% only on $\langle\bar{q}q\rangle^{1/3}_{n_f=3}/\bar{\Lambda}_3$. The effect appears slightly more pronounced—about a 7% relative reduction from $n_f=2$ to $n_f=3$—when comparing the central values of Eqs. (6.8) and (6.10), due to the slight 4% reduction of the (central) F_0 relative to F, although this result is not clear as it is affected by rather large uncertainties. We may finally combine Eqs. (6.8) and (6.10) to give

$$\begin{aligned}\frac{\langle\bar{q}q\rangle^{1/3}_{\mathrm{RGI},n_f=3}}{\langle\bar{q}q\rangle^{1/3}_{\mathrm{RGI},n_f=2}} &\simeq (0.97\pm0.01)\frac{\bar{\Lambda}_3}{\bar{\Lambda}_2}\\ &\simeq (0.94\pm0.01\pm0.12)\frac{F_0}{F}\\ &\simeq 0.86\pm0.01\pm0.11\pm0.05, \qquad (6.11)\end{aligned}$$

where all of our theoretical errors are combined linearly. In the results on the rhs of Eq. (6.11) the first quoted errors are the intrinsic RGOPT errors for the present condensate calculation only, and the second larger one is propagated from the $F/\bar{\Lambda}_2$ and $F_0/\bar{\Lambda}_3$ RGOPT theoretical errors. We also stress that in Eq. (6.11) our results are by construction in the strict chiral limit $m_q\to 0$. The result given for the unspecified F_0/F corresponds to the present sole RGOPT condensate estimate without extra input from other methods, while the last result uses the present lattice F_0/F estimates [2] (with its own uncertainty ∼0.05 quoted last).

B. Comparison and discussion

One may compare Eqs. (6.4) and (6.5) with the latest (presently most) precise lattice determination from the spectral density [13] for $n_f=2$: $\langle\bar{q}q\rangle^{1/3}_{n_f=2}(\mu=2\ \mathrm{GeV}) = -(261\pm6\pm8)$, where the first error is statistical and the second is systematic. Our results in Eq. (6.4) are thus compatible within uncertainties, though only marginally if taking the other RGOPT determination of $\bar{\Lambda}_2$ in Eq. (6.5), which tends to be relatively high. Note however that the above-quoted lattice value from Ref. [13] was obtained by fixing the scale with the F_K decay constant rather than using $\bar{\Lambda}$ (moreover with F_K being determined in the quenched approximation). It is thus probably more judicious to compare our results for the RG-invariant ratio (6.8) with theirs [13]: $2.77\pm0.02\pm0.04$. Overall, recent lattice determinations from various other methods roughly lie in the range $\langle\bar{q}q\rangle^{1/3}_{n_f=2}\sim -(220\text{–}320)$ MeV for $n_f=2$ [2], and quite similarly for $n_f=3$. The most precise lattice $n_f=3$ determination we are aware of is $\langle\bar{q}q\rangle^{1/3}_{n_f=3}(2\ \mathrm{GeV}) = -(245\pm16)$ MeV [49]. Concerning the $n_f=3$ to $n_f=2$ condensate ratio, various lattice results still have rather large uncertainties at present [2], but some recent results are compatible with a ratio of unity [50]. Our results compare a bit better with the latest ones from spectral sum rules [3]: $\langle\bar{u}u\rangle^{1/3}\sim -(276\pm7)$ MeV (and for the ratio [51,52], $\langle\bar{s}s\rangle/\langle\bar{u}u\rangle = 0.74^{+0.34}_{-0.12}$). However the sum rules method [3] actually precisely determines the current quark masses, extracting then the $\langle\bar{u}u\rangle$ value indirectly from using the exact GMOR relation ([1]).

We stress again the rather moderate n_f dependence of our result. This is in some tension with the larger estimated difference between the $n_f=2$ and $n_f=3$ cases obtained by some authors [18]. Since our results are by construction valid in the strict chiral limit, taken at face value they indicate that the possibly larger difference obtained by some other determinations is more likely due to the explicit breaking from the large strange-quark mass, rather than an intrinsic n_f dependence property of the condensate in the exact chiral limit.

VII. SUMMARY AND CONCLUSION

We have adapted and applied our RGOPT method to the perturbative expression of the spectral density of the Dirac operator, the latter being first obtained from the perturbative logarithmic discontinuities of the quark condensate in the $\overline{\mathrm{MS}}$ scheme. This construction allows for successive sequences of optimized nontrivial results in the strict chiral limit at two-, three-, and four-loop levels. These results exhibit a remarkable stability and empirical convergence. The intrinsic theoretical error of the method, taken as the difference between the three- and four-loop results, is of order 2%, while the final condensate value uncertainty is more affected by the present uncertainties on the basic QCD scale $\bar{\Lambda}$, especially with a larger uncertainty for $n_f=2$ flavors. The values obtained are rather compatible (within uncertainties) with the most recent lattice and sum rules determinations for $n_f=2$, and our values indicate a moderate flavor dependence of the $\langle\bar{q}q\rangle^{1/3}_{n_f}/\bar{\Lambda}_{n_f}$ ratio.

[1] M. Gell-Mann, R. J. Oakes, and B. Renner, Phys. Rev. **175**, 2195 (1968).
[2] G. Colangelo *et al.*, Eur. Phys. J. C **71**, 1695 (2011); S. Aoki *et al.*, Eur. Phys. J. C **74**, 2890 (2014).
[3] S. Narison, Phys. Lett. B **738**, 346 (2014).
[4] Y. Nambu and G. Jona-Lasinio, Phys. Rev. **122**, 345 (1961).
[5] S. P. Klevansky, Rev. Mod. Phys. **64**, 649 (1992); T. Hatsuda and T. Kunihiro, Phys. Rep. **247**, 221 (1994).
[6] P. Maris, C. D. Roberts, and P. C. Tandy, Phys. Lett. B **420**, 267 (1998); P. Maris and C. D. Roberts, Phys. Rev. C **56**, 3369 (1997).
[7] K. Langfeld, H. Markum, R. Pullirsch, C. D. Roberts, and S. M. Schmidt, Phys. Rev. C **67**, 065206 (2003).
[8] See, e.g., H. G. Dosch and S. Narison, Phys. Lett. B **417**, 173 (1998); M. Jamin, Phys. Lett. B **538**, 71 (2002).
[9] M. A. Shifman, A. I. Vainshtein, and V. I. Zakharov, Nucl. Phys. **B147**, 385 (1979).
[10] See, e.g., D. Becirevic and V. Lubicz, Phys. Lett. B **600**, 83 (2004); P. Hernandez, K. Jansen, L. Lellouch, and H. Wittig, J. High Energy Phys. 07 (2001) 018; A. Duncan, S. Pernice, and J. Yoo, Phys. Rev. D **65**, 094509 (2002).
[11] E. Marinari, G. Parisi, and C. Rebbi, Phys. Rev. Lett. **47**, 1795 (1981).
[12] L. Del Debbio, L. Giusti, M. Lüscher, R. Petronzio, and N. Tantalo, J. High Energy Phys. 02 (2006) 011; L. Giusti and M. Lüscher, J. High Energy Phys. 03 (2009) 013; H. Fukaya, S. Aoki, T. W. Chiu, S. Hashimoto, T. Kaneko, J. Noaki, T. Onogi, and N. Yamada, Phys. Rev. Lett. **104**, 122002 (2010); **105**, 159901(E) (2010).
[13] G. P. Engel, L. Giusti, S. Lottini, and R. Sommer, Phys. Rev. D **91**, 054505 (2015).
[14] T. Banks and A. Casher, Nucl. Phys. **B169**, 103 (1980).
[15] J. Gasser and H. Leutwyler, Ann. Phys. (N.Y.) **158**, 142 (1984); Nucl. Phys. **B250**, 465 (1985).
[16] H. Leutwyler and A. V. Smilga, Phys. Rev. D **46** (1992) 5607.
[17] A. V. Smilga and J. Stern, Phys. Lett. B **318**, 531 (1993); K. Zyablyuk, J. High Energy Phys. 06 (2000) 025.
[18] S. Descotes-Genon, L. Girlanda, and J. Stern, J. High Energy Phys. 01 (2000) 041; S. Descotes-Genon and J. Stern, Phys. Lett. B **488**, 274 (2000); S. Descotes-Genon, N. H. Fuchs, L. Girlanda, and J. Stern, Eur. Phys. J. C **34**, 201 (2004); V. Bernard, S. Descotes-Genon, and G. Toucas, J. High Energy Phys. 01 (2011) 107; 06 (2012) 051; M. Kolesar and J. Novotny, arXiv:1409.3380.
[19] J. Bijnens and T. A. Lahde, Phys. Rev. D **71** (2005) 094502.
[20] J.-L. Kneur and A. Neveu, Phys. Rev. D **81**, 125012 (2010).
[21] J.-L. Kneur and A. Neveu, Phys. Rev. D **85**, 014005 (2012).
[22] J.-L. Kneur and A. Neveu, Phys. Rev. D **88**, 074025 (2013).
[23] C. Arvanitis, F. Geniet, J. L. Kneur, and A. Neveu, Phys. Lett. B **390**, 385 (1997).
[24] J.-L. Kneur, Phys. Rev. D **57**, 2785 (1998).
[25] V. I. Yukalov, Theor. Math. Phys. **28**, 652 (1976); W. E. Caswell, Ann. Phys. (N.Y.) **123**, 153 (1979); I. G. Halliday and P. Suranyi, Phys. Lett. **85B**, 421 (1979); P. M. Stevenson, Phys. Rev. D **23**, 2916 (1981); Nucl. Phys. **B203**, 472 (1982); J. Killinbeck, J. Phys. A **14**, 1005 (1981); R. P. Feynman and H. Kleinert, Phys. Rev. A **34**, 5080 (1986); A. Okopinska, Phys. Rev. D **35**, 1835 (1987); A. Duncan and M. Moshe, Phys. Lett. B **215**, 352 (1988); H. F. Jones and M. Moshe, Phys. Lett. B **234**, 492 (1990); A. Neveu, Nucl. Phys. B, Proc. Suppl. **18**, 242 (1991); V. Yukalov, J. Math. Phys. (N.Y.) **32**, 1235 (1991); S. Gandhi, H. F. Jones, and M. Pinto, Nucl. Phys. **B359**, 429 (1991); C. M. Bender, F. Cooper, K. A. Milton, M. Moshe, S. S. Pinsky, and L. M. Simmons, Phys. Rev. D **45**, 1248 (1992); S. Gandhi and M. B. Pinto, Phys. Rev. D **46**, 2570 (1992); H. Yamada, Z. Phys. C **59**, 67 (1993); K. G. Klimenko, Z. Phys. C **60**, 677 (1993); A. N. Sissakian, I. L. Solovtsov, and O. P. Solovtsova, Phys. Lett. B **321**, 381 (1994); H. Kleinert, Phys. Rev. D **57**, 2264 (1998); Phys. Lett. B **434**, 74 (1998); Phys. Rev. D **60**, 085001 (1999); Mod. Phys. Lett. B **17**, 1011 (2003).
[26] C. Arvanitis, F. Geniet, M. Iacomi, J.-L. Kneur, and A. Neveu, Int. J. Mod. Phys. A **12**, 3307 (1997).
[27] R. Seznec and J. Zinn-Justin, J. Math. Phys. (N.Y.) **20**, 1398 (1979); J. C. Le Guillou and J. Zinn-Justin, Ann. Phys. (N.Y.) **147**, 57 (1983); J. Zinn-Justin, arXiv:1001.0675.
[28] R. Guida, K. Konishi, and H. Suzuki, Ann. Phys. (N.Y.) **241**, 152 (1995); **249**, 109 (1996).
[29] J.-L. Kneur and D. Reynaud, Phys. Rev. D **66**, 085020 (2002).
[30] H. Kleinert, Mod. Phys. Lett. B **17**, 1011 (2003); B. Kastening, Phys. Rev. A **68**, 061601 (2003); **69**, 043613 (2004).
[31] J.-L. Kneur, A. Neveu, and M. B. Pinto, Phys. Rev. A **69**, 053624 (2004).
[32] J. L. Kneur, M. B. Pinto, R. O. Ramos, and E. Staudt, Phys. Rev. D **76**, 045020 (2007).
[33] J. L. Kneur, M. B. Pinto, and R. O. Ramos, Phys. Rev. C **81**, 065205 (2010).
[34] J. A. M. Vermaseren, S. A. Larin, and T. van Ritbergen, Phys. Lett. B **405**, 327 (1997); K. G. Chetyrkin, Nucl. Phys. **B710**, 499 (2005); M. Czakon, Nucl. Phys. **B710**, 485 (2005).
[35] B. Hamprecht and H. Kleinert, Phys. Rev. D **68**, 065001 (2003).
[36] D. J. Gross and A. Neveu, Phys. Rev. D **10**, 3235 (1974).
[37] MATHEMATICA, version 6, Wolfram Research.
[38] K. G. Chetyrkin and V. P. Spiridonov, Yad. Fiz. **47**, 818 (1988) [Sov. J. Nucl. Phys. **47**, 522 (1988)].
[39] K. G. Chetyrkin and J. H. Kühn, Nucl. Phys. **B432**, 337 (1994); K. G. Chetyrkin and A. Maier, J. High Energy Phys. 01 (2010) 092.
[40] J. C. Collins, *Renormalization. An Introduction To Renormalization, The Renormalization Group, And The Operator Product Expansion* (Cambridge University Press, Cambridge, England, 1984).
[41] K. G. Chetyrkin and A. Maier (private communication).
[42] T. Inagaki, D. Kimura, and A. Kvinikhidze, Phys. Rev. D **77**, 116004 (2008).
[43] K. G. Chetyrkin, J. H. Kuhn, and M. Steinhauser, Comput. Phys. Commun. **133**, 43 (2000).
[44] See the QCD review chapter by K. A. Olive *et al.* (Particle Data Group Collaboration), Chin. Phys. C **38**, 090001 (2014).
[45] B. Blossier, Ph. Boucaud, F. De soto, V. Morenas, M. Gravina, O. Pène, and J. Rodríguez-Quintero (ETM Collaboration), Phys. Rev. D **82**, 034510 (2010).
[46] K. G. Chetyrkin, B. A. Kniehl, and M. Steinhauser, Phys. Rev. Lett. **79**, 2184 (1997); Nucl. Phys. **B510**, 61 (1998); K. G.

Chetyrkin, J. H Kühn, and C. Sturm, Nucl. Phys. **B744**, 121 (2006).
[47] F. Karbstein, A. Peters, and M. Wagner, J. High Energy Phys. 09 (2014) 114.
[48] K. Jansen, F. Karbstein, A. Nagy, and M. Wagner (ETM Collaboration), J. High Energy Phys. 01 (2012) 025.
[49] A. Bazavov *et al.*, *Proc. Sci.*, CD09 (2009) 007, arXiv:0910.2966.
[50] C. T. H. Davies, C. McNeile, A. Bazavov, R. J. Dowdall, K. Hornbostel, G. P. Lepage, and H. Trottier, *Proc. Sci.*, ConfinementX (2012) 042.
[51] C. A. Dominguez, N. F. Nasrallah, R. Rontsch, and K. Schilcher, J. High Energy Phys. 05 (2008) 020.
[52] S. Narison and R. Albuquerque, Phys. Lett. B **694**, 217 (2010); R. M. Albuquerque, S. Narison, and M. Nielsen, Phys. Lett. B **684**, 236 (2010).